Plant Cell Physiol. 48(6): 804–811 (2007)
doi:10.1093/pcp/pcm048, available online at www.pcp.oxfordjournals.org

A Grape Berry (*Vitis vinifera* L.) Cation/Proton Antiporter is Associated with Berry Ripening

Mohsen Hanana [1,2], Olivier Cagnac [2], Toshio Yamaguchi [2], Saïd Hamdi [3], Abdelwahed Ghorbel [1] and Eduardo Blumwald [2,*]

[1] *Laboratoire de Physiologie Moléculaire de la Vigne, INRST, BP 901, Hammam-lif 2050, Tunisia*
[2] *Department of Plant Sciences, University of California, One Shields Ave, Davis, CA 95616, USA*
[3] *Laboratoire de Génomique Fonctionnelle et de la Qualité de la Baie de Raisin, Université de Bordeaux 1, 71 Av. Edouard Bourleaux, BP 81, 33883Bordeaux, France*

We have cloned and characterized *VvNHX1*, a gene encoding a vacuolar cation/H^+ antiporter from *Vitis vinifera* cv. Cabernet Sauvignon. VvNHX1 belongs to the vacuolar NHX protein family and showed high similarity to other known vacuolar antiporters. The expression of *VvNHX1* partially complements the salt- and hygromycin-sensitive phenotypes of an *ena1-4 nhx1* yeast strain. Immunoblots of vacuoles of yeast expressing a VvNHX1, together with the expression of a *VvNHX1–GFP* (green fluorescent protein) chimera demonstrated that VvNHX1 localized to the vacuoles. VvNHX1 displayed low affinity K^+/H^+ and Na^+/H^+ exchange activities (12.8 and 40.2 mM, respectively). The high levels of expression of *VvNHX1* during the véraison and post-véraison stages would indicate that the increase in vacuolar K^+ accumulation, mediated by VvNHX1, is needed for vacuolar expansion. This process, together with the rapid accumulation of reducing sugars, would drive water uptake to the berry and the concomitant berry size increase, typical of the post-véraison stage of growth.

Keywords: Cation/H^+ antiporter — Grape berry — NHX — Vacuole — Véraison — *Vitis vinifera*.

Abbreviation: EST, expressed sequence tag; GFP, green fluorescent protein; ORF, open reading frame; RT–PCR, reverse transcription–PCR.

The nucleotide sequence reported in this paper has been submitted to GenBank under accession number AY634283.

Introduction

During development, grape berries display two successive periods of swelling and active growth (green and ripening stage) that are separated by a phase of slow growth (Kanellis and Roubelakis-Angelakis 1993). Initially, during the first period of growth, called the green stage, organic acids (mainly tartaric and malic acids) accumulate in the berry with the concomitant acidification of the berry to a pH of around 2.5 (Ruffner 1982). The second phase of berry growth starts with the onset of ripening (i.e. the véraison phase), and is characterized by cell expansion with the accumulation of sugars and amino acids and a relative decrease in acid content, mostly due to the breakdown of malate (Ruffner 1982). The volume of the grape berry is largely occupied by a central vacuole, and the transport of ions and sugars across the vacuolar membrane plays a paramount role in cell expansion and berry development. Two berry vacuolar H^+ pumps, an inorganic pyrophosphatase (H^+-PPase, EC 3.6.1.1) and an H^+-ATPase (EC 3.6.1.3), have been characterized (Terrier et al. 2001). These H^+ pumps establish the electrochemical proton gradient that drives the secondary active transport of inorganic ions, organic acids and sugars into the vacuole of the grape berry (Blumwald 1987). A number of grape berry vacuolar transporters have been identified. Plasma membrane aquaporins (Picaud et al. 2003), sugar transporters (Manning et al. 2001, Atanassova et al. 2003) and grape guard cell K^+ channels (Pratelli et al. 2002) have been functionally characterized, and the two genes encoding KUP/KT/HAK-type potassium transporters that are expressed in grape have been described (Davies et al. 2006). Nevertheless, data on the mechanisms of solute and ion accumulation in grape berry vacuoles are scanty. Although several expressed sequence tags (ESTs) encoding putative vacuolar transporters have been identified in the databases, there is no functional assessment of their putative role. The grape berry vacuoles maintain an acidic pH ranging from pH 2.5 in the green stage to pH 3.5 during ripening, and the maintenance of vacuolar ion concentration gradients and pH is essential for the acid and sugar homeostasis in the berry. Thus, the efficient regulation of the vacuolar pH and the transport of counterbalancing cations are essential processes to maintain ion and sugar concentrations that are optimal for growth and development. The NHX-type vacuolar cation/H^+ antiporters couple the passive movement of H^+ out of the vacuole to the active movement of monovalent cations (mainly K^+ and Na^+) (Pardo et al. 2006) into the vacuole. Plant NHX-type vacuolar cation/H^+ antiporters have been shown to be involved in a number of

*Corresponding author: E-mail, eblumwald@ucdavis.edu; Fax, +1-530-752-2278.

cellular processes, including the transport of K^+ and Na^+ ions into the plant vacuole (Apse et al. 1999, Zhang and Blumwald, 2001), the regulation of vacuolar pH (Yamaguchi et al. 2001), vesicular trafficking (Sottosanto et al. 2004), and so on.

Here, we describe the cloning and functional characterization of VvNHX1, a grapevine vacuolar Na^+/H^+ antiporter. Measurements of VvNHX1 activity, together with its expression profiles during development, support the role of VvNHX1 in vacuolar ion homeostasis in grape berries.

Results

Cloning and molecular characterization of VvNHX1

The cloned cDNA of *VvNHX1* is 2,053 nucleotides long, with a 5′-untranslated region of 60 nucleotides, a predicted open reading frame (ORF) of 1,626 nucleotides and a 3′-untranslated region of 367 nucleotides. The predicted ORF encodes a protein of 541 amino acids with a calculated molecular mass of 60 kDa that shared similarities with other NHX-type vacuolar Na^+/H^+ antiporters. The phylogenetic tree (Fig. 1) shows that VvNHX1 is most closely related to InNHX1, PhNHX and NcNHX from *Ipomoea nil*, *Petunia hybrida* and *Nierenbergia caerulea*, respectively. It is noteworthy that these cDNAs were all obtained from flowers (Ohnishi et al. 2005). Similarly to other higher plant vacuolar NHX proteins, VvNHX1 contained the highly conserved 10-transmembrane segments, as revealed by transmembrane prediction programs (TMHMM, DAS, PRED-TMR, TMpred, SMART and toppred) and a putative amiloride-binding domain (^{84}LFFIYLLPPI^{93}) in the third transmembrane region.

Heterologous expression of VvNHX1 in yeast and functional complementation

The heterologous complementation of *Saccharomyces cerevisiae* mutants with plant genes provides a useful system to assess plant protein functions. Because of the similarity between ScNhx1, the yeast endosomal Na^+/H^+ antiporter, and plant vacuolar antiporters, yeast mutants lacking ScNHX1 provide a unique tool for the assessment of the functional role of plant NHX-like proteins (Quintero et al. 2000, Yokoi et al. 2002, Aharon et al. 2003). The *VvNHX1* ORF was placed under the control of a constitutive promoter for the expression of the heterologous protein in yeast. Experiments were carried out to determine whether the *VvNHX1* gene product could functionally complement the *ena 1-4 nhx1* yeast mutant (Aharon et al. 2003) by suppressing its observed phenotypes. Expression of *VvNHX1* partially restored the ability of the *ena 1-4 nhx1* mutant to grow in the presence of hygromycin (Fig. 2a).

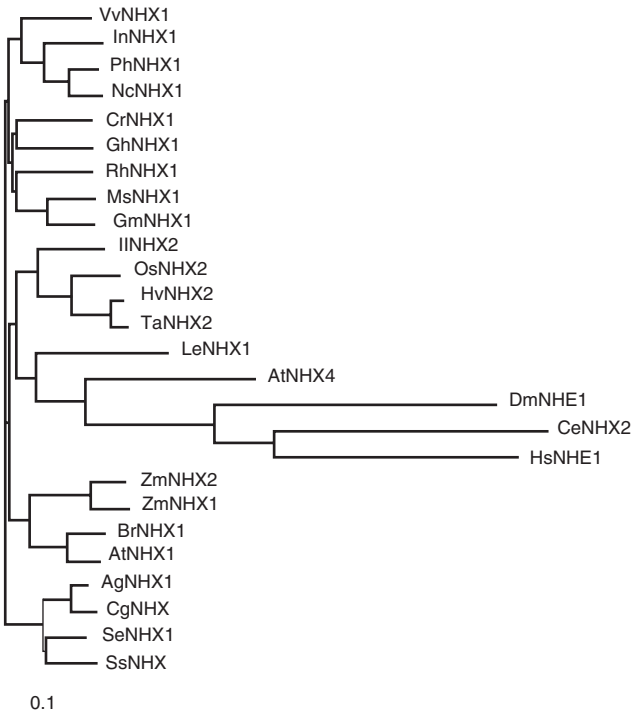

Fig. 1 Phylogenetic tree of NHX-like vacuolar cation/H^+ antiporters. VvNHX1, *Vitis vinifera* (AAV36562); PhNHX1, *Petunia hybrida* (BAB56105); CrNHX1, *Citrus reticulata* (AAT36679); NcNHX, *Nierembergia caerulea* (BAB56106); MsNHX, *Medicago sativa* (AAR19085); InNHX1, *Ipomoea nil* (BAD91201); GhNHX1, *Gossypium hirsutum* (AAM54141); GmNHX, *Glycine max* (AAR27596); IlNHX2, *Iris lactea* (AAU81619); AgNHX1, *Atriplex gmelini* (BAB11940); RhNHX, *Rosa hybrida* (BAD93487); SeNHX1, *Salicornia europaea* (AAN08157); CgNHX, *Chenopodium glaucum* (AAQ72785); SsNHX, *Suaeda maritima* subsp. salsa (AAK53432); HvNHX1, *Hordeum vulgare* (BAC56698); OsNHX1, *Oryza sativa* (AAQ74383); TaNHX2, *Triticum aestivum* (AAK76738); ZmNHX2, *Zea mays* (AAP20429); BrNHX1, *Brassica napus* (AAO38856); ZmNHX1, *Zea mays* (AAP20428); LeNHX1, *Lycopersicon esculentum* (CAC84522); AtNHX4, *Arabidopsis thaliana* (AAM08405); DmNHE1, *Drosophila melanogaster* (AAD32689); CeNHX2, *Caenorhabditis elegans* (AAA62524); AtNHX1, *Arabidopsis thaliana* (AAD16946); HsNHE1, *Homo sapiens* (AAF25592).

In addition, expressing *VvNHX1* in the *ena 1-4 nhx1* mutant significantly improved the ability of the mutant to grow in the presence of 180 mM NaCl and 5 mM LiCl (Fig. 2b, c). These results indicated that VvNHX1 was at least partially able to replace the yeast nhx1 function.

To determine the localization of VvNHX1 in yeast, cells were transformed with constructs bearing green fluorescent protein (GFP)-tagged VvNHX1 or GFP alone (Fig. 3). In cells expressing GFP alone, the GFP fluorescence was seen mainly in the cytosol (Fig. 3a–c), whereas, in cells expressing VvNHX1::GFP, the fluorescence was seen both in the vacuole and in the small vesicular organelles (Fig. 3d–f). The vacuolar localization of VvNHX1 was also

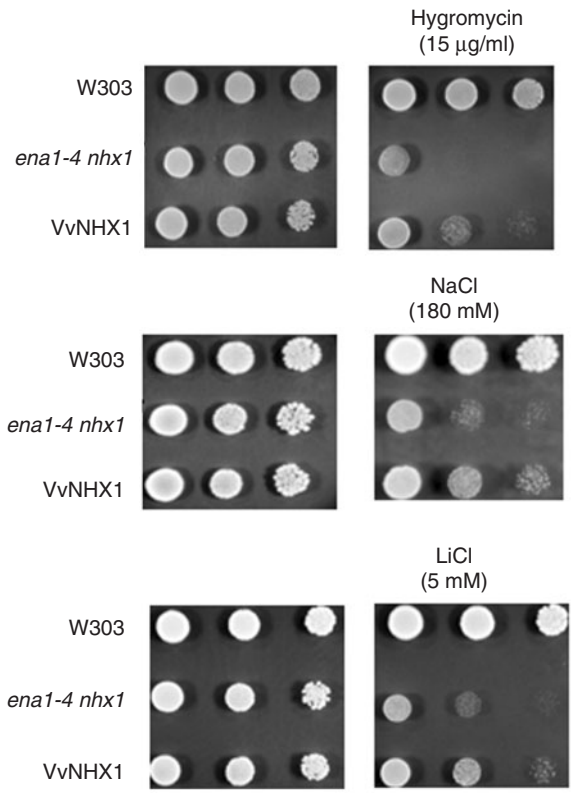

Fig. 2 Complementation of the hygromycin- and salt-sensitive phenotype of the *Saccharomyces cerevisieae* mutant *ena 1-4 nhx1* by VvNHX1. Three serial dilutions (1 : 10; 1 : 100; 1 : 1,000) of saturated cultures were spotted onto APG solid media at pH 5.5 supplemented with 15 µM hygromycin (a), 180 mM NaCl (b) or 5 mM LiCl (c). Growth of the colonies was assessed after 2 d at 30°C. The pYPGE15 empty vector was introduced into the *S.cerevisieae* W303 strain.

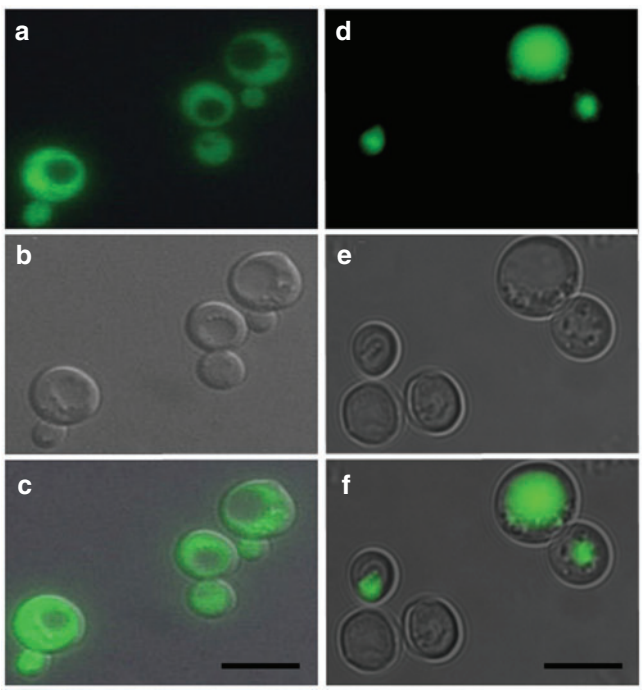

Fig. 3 Localization of VvNHX1–GFP to yeast vacuoles. Yeast cells carrying the pDR196-*VvNHX1–GFP* were grown at 30°C to the logarithmic growth phase and observed by fluorescence microscopy. (a) Fluorescence of yeast cells transformed with pDR196–*GFP* alone; (b) contrasted images; (c) overlay of fluorescence and contrasted images; (d) fluorescence of yeast cells transformed with pDR196-*VvNHX1–GFP*; (e) contrasted images; (f) overlay of fluorescence and contrasted images. Bar = 5 µm.

assessed by Western blots of yeast intact vacuoles expressing FLAG-tagged VvNHX1 (Fig. 4). Immunoblotting of vacuoles isolated from untransformed W303 yeast cells and cells transformed with VvNHX1-FLAG revealed the presence of the fusion protein with an apparent molecular mass of approximately 50 kDa in the vacuolar membranes of yeast expressing VvNHX1-FLAG. The apparent molecular mass (50 kDa) is somewhat lower than that predicted by the amino acid sequence of the VvNHX1 ORF (60 kDa) and may reflect anomalous migration in SDS–PAGE; anomalies in the apparent molecular mass similar to those detected by SDS–PAGE have been reported for other Na^+/H^+ exchangers (Numata et al. 1998, Apse et al. 1999).

VvNHX1 mediates Na^+/H^+- and K^+/H^+-coupled exchange

The functional complementation of the *S. cerevisiae nhx1* mutant strains by *VvNHX1* expression and the localization of VvNHX1 in the yeast vacuole made possible the study of the transport properties of VvNHX1. This was performed by comparing transport in vacuoles isolated from yeast expressing *VvNHX1* and expressing the transformation vector alone. $Cation^+/H^+$ antiporter activity was assayed by measuring the rates of cation-dependent H^+ efflux using fluorescence quenching (Blumwald 1987, Yamaguchi et al. 2003). For both Na^+ and K^+, the H^+-dependent cation exchange mediated by VvNHX1 displayed simple Michaelis–Menten kinetics (Fig. 5a). The VvNHX1 transport activity saturated with increasing concentrations of Na^+ and K^+, with apparent affinity constants (K_m) of approximately 40 and 13 mM respectively (Table 1), and similar apparent V_{max} values, thus suggesting a higher affinity for K^+ than for Na^+ (Fig. 5b).

Expression of VvNHX1 during berry development

Reverse transcription–PCR (RT–PCR) was used to examine *VvNHX1* expression during berry development (Fig. 6). Our results showed that *VvNHX1* transcripts could not be detected at the early stages of berry development, i.e. at 20 and 40 d after flowering (B1 and B2, respectively), or in the green skin (GS). High levels of transcripts were detected in the berry flesh after the véraison stage (70 d after flowering), to a lesser extent at 100 and 120 d

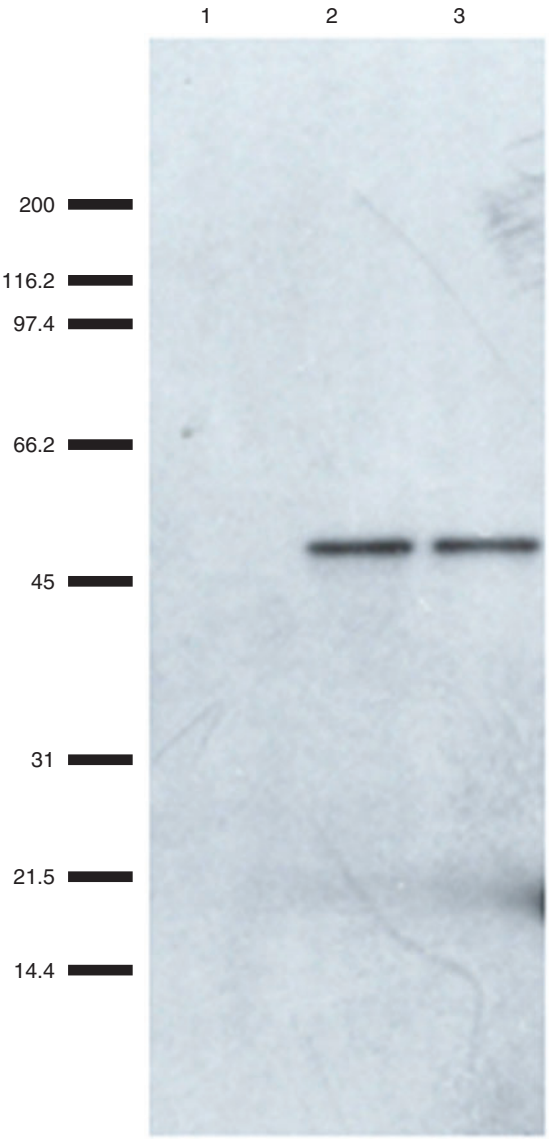

Fig. 4 Immunodetection of VvNHX1 in yeast cells. Lane 1, total microsomal membranes of W303 cells transformed with empy plasmid. Lane 2, total microsomal membranes of *S. cereviseae* expressing VvNHX1. Lane 3, tonoplast proteins isolated from *S. cereviseae* expressing VvNHX1. Molecular masses are indicated at the left of the figure.

after flowering (B4 and B5, respectively), and low transcript amounts were detected in the red skin tissue (RS). On the other hand, no transcripts were detected in young and old leaves and roots, suggesting that VvNHX1 expression was specific in the berry flesh (Fig. 6).

Discussion

We have identified VvNHX1, a novel grapevine vacuolar Na^+/H^+ antiporter belonging to the NHX-type of transporters. These transporters have been identified in a large number of different plant species, including gymnosperms and monocotyledonous and dicotyledonous angiosperms (Pardo et al., 2006). In general, *VvNHX1* showed high sequence similarity to other plant and yeast vacuolar NHX-type genes and phylogenetically belongs to a group comprising genes from ornamental plants such as *I. nil*, *P. hybrida* and *N. caerulea*. VvNHX1 displayed similar characteristics to other NHX-like proteins; an amiloride-binding domain in the putative transmembrane domain 3, an N-terminal hydrophobic domain comprised of approximately 440 amino acids, with 10–12 putative transmembrane domains and a hydrophilic C-terminal domain with 100 amino acids which appears to be involved in the regulation of the antiporter activity and cation selectivity (Yamaguchi et al. 2003, Yamaguchi et al. 2005). The expression of *VvNHX1* suppressed the Na^+-, Li^+- and hygromycin-sensitive phenotypes of the yeast mutant lacking the endosomal/vacuolar Na^+/H^+ antiporter and the plasma membrane Na^+-ATPase (*Δnhx1,Δena1-4*), although the cells expressing *VvNHX1* displayed a lower tolerance for Na^+, Li^+ and hygromycin than those of the wild-type cells. Similar partial complementation has been reported for *AtNHX1* (Gaxiola et al. 1999), *AgNHX1* (Hamada et al. 2001), *OsNHX1* (Fukuda et al. 2004), *BvNHX1* (Xia et al. 2002), *TNHX1* (Brini et al. 2005) and other plant NHX-like genes, supporting the notion that VvNHX1 was functional in our complementation assays and that it localized in the vacuolar/pre-vacuolar compartments. This was confirmed by immunoblots from yeast cells expressing a FLAG-tagged VvNHX1; antibodies raised against the FLAG tag only reacted with proteins and vacuoles from yeast cells expressing a FLAG-tagged VvNHX1. Further confirmation supporting the vacuolar localization of VvNHX1 in yeast was provided by fluorescence microscope studies of yeast cells expressing a GFP–VvNHX1 fusion protein.

Vacuolar NHX-like cation$^+/H^+$ antiporters have been shown to play significant cellular roles, including cell expansion and K^+ homeostasis (Apse et al. 2003), intravacuolar pH regulation and cellular pH homeostasis (Yamaguchi et al. 2001), and vesicular trafficking (Sottosanto et al. 2004). Increasing evidence supports the notion that in glycophytes, NHX-like proteins mediate the accumulation of K^+ ions in the vacuole and also provide homeostatic control of cytosolic K^+ concentrations (Pardo et al. 2006). Experiments with Arabidopsis *nhx1* knockout plants showed altered leaf development and reduced leaf expansion, indicating the important role of the vacuolar antiporters in net K^+ uptake and turgor-driven cell growth (Apse et al. 2003). Grape berries are a strong sink for K^+ ions, and K^+ is the major cation accumulated in the berries, reaching amounts higher than 3 mg g FW^{-1} berry

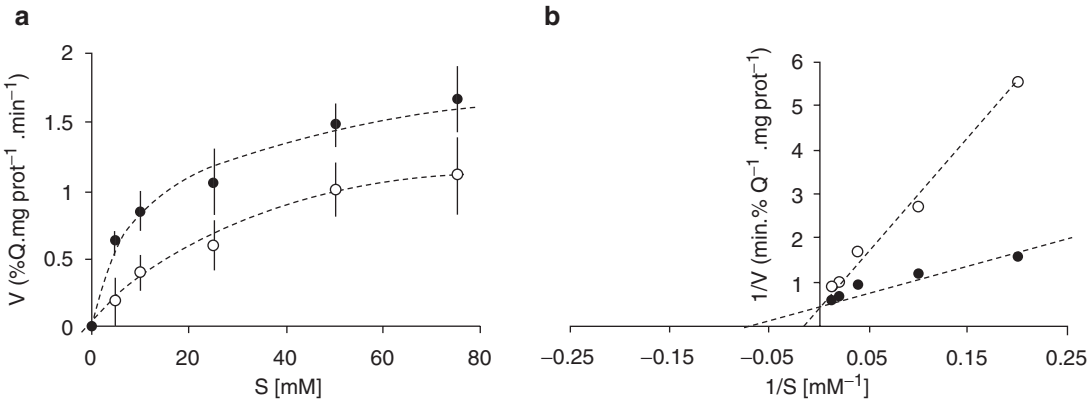

Fig. 5 Cation/H^+ exchange mediated by VvNHX1. (a) Initial rates of cation-dependent H^+ movements were assayed by measuring the initial rates of fluorescence quench recovery after addition of NaCl or KCl, as indicated in Materials and Methods. Filled circles, K^+; open circles, Na^+. Values are the mean ± SD ($n = 5$). (b) Double reciprocal plot of the K^+- and Na^+-dependent H^+ fluxes. The lines are those of best fit by the least squares method.

Table 1 Kinetics of Na^+/H^+ and K^+/H^+ exchange of vacuoles harboring VvNHX1

	Na^+	K^+	Na^+/K^+
V_{max} (%Q/mg protein min)	1.72 ± 0.18	1.85 ± 0.15	0.93
K_m (mM)	40.23 ± 9.14	12.85 ± 3.35	

Values are the mean ± SD ($n = 6$–8).

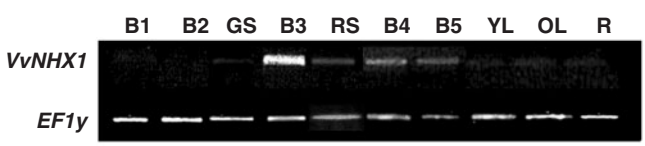

Fig. 6 *VvNHX1* expression during *Vitis vinifera* berry development. RT–PCR was performed as described in Materials and Methods. Elongation factor-1γ (Ef1γ) was used as an internal control to normalize expression of *VvNHX1*. B1 and B2, green berry (20 and 40 d after flowering, respectively); B3, véraison stage; B4 and B5, red berry (100 and 1,200 d after flowering, respectively); S2 and S4, green skin and red skin, respectively; YL, young leaves; OL, old leaves; R, roots.

(3,000 p.p.m.) (Hrazdina et al. 1984, Rogiers et al. 2000). Potassium is considered to be a phloem-mobile element (Welch 1986) and continues to accumulate in the grape berry throughout development via phloem flow into the grape berries. A key role for K^+ ions in cell expansion is supported by results showing that K^+ accumulated predominantly in the pulp and skin tissues, and a high correlation between K^+ accumulation and berry fresh weight (Rogiers et al. 2006).

The growth pattern of grape berries follows a double-sigmoid curve (Kanellis and Roubelakis-Angelis 1993). In the first stage, the berry's size increases rapidly mainly due to cell division, followed by cell expansion (Mpelasoka et al. 2003, and references therein). Two types of K^+ transporters have been associated with this stage of growth. Grapevine stomatal inward rectifying K^+ (SIRK) channels were shown to be expressed in stomata and berries, and semi-quantitative RT–PCR showed that the transcripts encoding SIRK channels were detected mainly in the green berry, and that their expression decreased drastically by the time of véraison (Pratelli et al. 2002). Two potassium transporters from the KUP/KT/HAK family were identified in grape berry and their function demonstrated by functional complementation of *Escherichia coli* mutants (Davies et al. 2006). These transporters were highly expressed in the berry skin before véraison, suggesting their involvement in K^+ acquisition during the first stage of berry growth. The véraison stage is the beginning of fruit ripening and is characterized by softening and coloring of the berry. It precedes the second stage of growth that is associated with rapid growth which is due entirely to cell expansion, rapid accumulation of sugars and a sharp increase in K^+ content (Ollat and Gaudillere 1996, Mpelasoka et al. 2003). The high levels of expression of *VvNHX1* during the véraison and post-véraison stages would indicate that the increase in vacuolar K^+ accumulation, mediated by VvNHX1, is needed for vacuolar expansion. This process, together with the rapid accumulation of reducing sugars, would drive water uptake to the berry and the concomitant berry size increase, typical of the post-véraison stage of growth.

Grape EST sequence databases contain four contigs with sequence similar to *VvNHX1*, accession Nos. CTG1034112, CF201222, CTG1032616 and CTG1032768. While CTG1034112 and CF201222 EST contigs are identical to *VvNHX1*, CTG1032768 and CTG1032768 appear to encode other VvNHX-like cation/antiporters. The characterization of these transporters is in progress.

Materials and Methods

Identification and cloning of the VvNHX1 gene

Degenerate primers were designed for the cloning of an Na^+/H^+ antiporter from grapevine. We designed degenerate primers from conserved regions of different plant Na^+/H^+ antiporter sequences (not shown), and PCRs were performed on a berry cDNA library at the véraison stage. The two primers were: NHX1F, 5′-GCGACAGATTCTGTTTGCAC-3′; and NHX1R, 5′-AGGACTGGATGGTTCAGAAG-3′. The conditions for amplification were 94°C for 3 min followed by 30 cycles at 94°C for 1 min, 54°C for 30 s, 72°C for 2 min and 72°C for 10 min. The amplified fragment (≈900 bp length) was purified from agarose gels, ligated into the pGEMT-easy vector (Promega, Madison,WI, USA) and sequenced. On the basis of the fragment sequences, specific primers (VvNHX1F, 5′- CGACATTGTCATTTGTTGC-3′; and VvNHX1R, 5′-GCAACAAATGACAATGTCG-3′) and universal SP6 and T7 primers were used for asymmetric PCR on the cDNA library. The assembly of contiguous sequences provided a full-length cDNA (2.053 kb) named *VvNHX1* with an ORF of 1,626 nucleotides which has been deposited in GenBank (accession No. AY634283). The *VvNHX1* ORF was inserted into the *Eco*RI/*Sal*I site of the pDR196 shuttle vector which was used for complementation studies and transport assays in yeast. For vacuolar transport assays, the TY001 (*MATα pep4-3 prb1-1122 leu2 trp1 ura3-52 nhx1Δ*::*TRP1*) *nhx1* yeast mutant (Yamaguchi et al. 2003) was transformed with either the empty pDR196 plasmid or the pDR196 plasmid containing *VvNHX1*.

Yeast strains, media and growth conditions

The *S. cerevisiae* yeast strains used in the complementation studies, wild type and mutant (*Δena1-2::HIS3*,*Δnhx1::HIS3*), were isogenic to W303-1B (*MATα*, *ade2-1;ura3-1, can1-100, leu2-3, trp1-1, his3-11,15*). The wild type and mutant strains were transformed using the lithium acetate method (Gietz et al. 1995) with either an empty pDR196 plasmid or a pDR196 plasmid containing *VvNHX1* cDNA. For complementation studies, yeasts were grown at 30°C in YPD (1% yeast extract, 2% peptone, 2% D-glucose) or APG (synthetic minimal medium containing 10 mM arginine, 8 mM phosphoric acid, 2% glucose, 2 mM $MgSO_4$, 1 mM KCl, 0.2 mM $CaCl_2$, and trace minerals and vitamins). The pH was adjusted to 5.5 and 6.5 for APG and YPD, respectively. Exponentially grown cells were harvested and adjusted to $OD_{600} = 2.0$, and serial dilutions of 1/10, 1/100 and 1/1,000 were made. A 10 µl aliquot of each culture was spotted onto APG and YPD plates (Yamaguchi et al. 2003). Hygromycin, NaCl and LiCl were added as indicated. Growth of colonies was assessed after 2 d at 30°C.

VvNHX1–GFP localization

To analyze the subcellular localization of VvNHX1 protein by heterologous expression in yeast, chimera constructions were prepared using a modified GFP, mGFP6, by the introduction of two point mutations (conversion of Phe64 to leucine and Ser65 to threonine, F64L and S65T) to change the emission and the excitation characteristics of the protein (Haseloff 1999).

The cDNA fragments carrying the *VvNHX1* and *mGFP6* coding regions were amplified with the following primers: *VvNHX1* (excluding the termination codon), SpeI-VvNHXs 5′-ACTAGTATGGGGTTTGAATTAGGCTCTG-3′ and VvNHXmGFP6as (stop codon removed) 5′-TCTCCTTTACT CATGGATCCTCGCCATTGACCAAGGTTTGG-3′; mGFP6, VvNHXmGFP6s 5′-CCAAACCTTGGTCAATGGCGAGGATC CATGAGTAAAGGAGA-3′ and EcorImGFP6as 5′-GAATTCT CAAGATCTTTTGTATAG-3′.

These fragments were fused by PCR and then subcloned into the pGEMT-easy vector using the underlined *Spe*I and *Eco*RI restriction sites. Sequence fidelity of the *VvNHX-mGFP6* was confirmed by sequencing. For subcellular localization in yeast cells, the construct was cloned in the pDR196+URA3 yeast expression vector. As a positive control, the mGFP6 was cloned into the same vector for comparative purposes.

The W303-1B (*MATα*, *ade2-1;ura3-1, can1-100, leu2-3, trp1-1, his3-11,15*) strain was transformed with pDR196, a pCEN URA3 plasmid encoding VvNHX–mGFP6, and the mGFP6 control. Transformants were grown in 5 ml of SD medium (6.7 g l^{-1} yeast nitrogen base without amino acids, 1.92 g l^{-1} yeast synthetic drop-out medium supplemented without uracil) at 30°C to logarithmic phase. A drop of cell suspension was spread on a poly-L-lysine-treated coverslip and placed on a glass slide. A Leica DMR fluorescent microscope equipped with a Chroma 86013 filter set (Chroma Technology Corp., Rockingham, VT, USA) and Coolsnap-HQ (Roper Scientific, Inc., Tucson, AZ, USA) was used to visualize the yeast cells. Enhanced GFP (EGFP) was visualized using filters S484/15x and S517/30m, FM4-64 was visualized with S555/25x and S605/40m, and vacuolar autofluorescence was visualized using S360/40x and S457/17m. All images were taken at 200× magnification. Images were pseudo-colored and merged using Metamorph software (Universal Imaging Corp., Downingtown, PA, USA).

Total proteins extraction and Western blots

The C-terminal 3 × FLAG-tagged VvNHX1 construct was generated by a fusion PCR method and cloned into the *Sma*I site of pDR196, and then transformed into the TY001 (*MATα pep4-3 leu2 trp1 ura3-52 prb1-1122 nhx1Δ*::*TRP1*) yeast strain. Yeast cells were grown to 1 OD, cells were collected and total proteins were extracted by alkaline lysis followed by trichloroacetic acid precipitation as described by Benli et al. (1996). SDS–PAGE and Western blotting were performed as described previously (Laemmli 1970, Burnette 1981). For Western blot analysis, equal amounts of each sample were resolved on 10% SDS–polyacrylamide gels. Equal volumes of sample buffer containing 100 mM Tris–HCl pH 6.8, 4% SDS, 20% glycerol, 12% 2-mercaptoethanol and a trace of bromophenol blue were added to the protein samples. Then the samples were immediately loaded onto 10% polyacrylamide gels containing 0.1% SDS and separated. Proteins on the gel were transferred onto a PVDF membrane (Amersham Bioscience) by electroblotting. Immnunoblots were performed as described elsewhere (Yamaguchi et al. 2003) using a polyclonal FLAG antibody (Sigma-Aldrich) and anti-rabbit IgG antibodies conjugated to horseradish peroxidase (Molecular Probes). The blots were visualized by enhanced chemiluminescence (ECL) (Amersham Bioscience). For assessing the relative quantities of the loaded protein, the membranes were stained with Coomassie brilliant blue.

RT–PCR analysis

To study the expression of *VvNHX1* in berry tissue, *V. vinifera* cv Cabernet Sauvignon berries were harvested from a vineyard in Bordeaux between June and September in order to obtain different phenological stages of berry development. After cutting the pedicel, the flesh of the berries was separated from skin and seeds, immediately frozen in liquid nitrogen and then stored at –80°C until use. Roots and leaves were obtained from seedlings

grown under hydroponic conditions. For RNA extraction from berries, the protocol described by Asif et al. (2000) was used. RNA from roots and leaves was extracted using a protocol with cetyl trimethyl ammonium bromide (CTAB) and lithium chloride precipitation (Chang et al. 1993).

To remove the genomic DNA contamination, total RNA was treated with DNase I (Promega), extracted again by phenol/chloroform/isoamylalcohol, precipitated by sodium acetate and finally suspended in diethylpyrocarbonate (DEPC)-treated sterile water. For first-strand cDNA synthesis, reverse transcription was carried out with reverse transcriptase (100 U of MMLV RNase H, Promega) on 2 μg of total RNA (denaturated at 75°C for 10 min) for 60 min at 42°C in the presence of 1.2 μM oligo(dT), 5× RT buffer, 4 mM dithiothreitol (DTT), 800 μM dNTPs and 20 U of RNasin.

After completion of first-strand cDNA synthesis, 5 μl aliquots were taken for PCR. The detection of transcripts was done by using the forward primer 5′-GCGACAGATTCTGTTTGCAC-3′and reverse primer 5′-GTGCTGGTGATCATAACTGC-3′. The expected length of the amplified fragment is 900 bp. PCR comprised 25 cycles of 94°C for 1 min, 52°C for 30 s, and 72°C for 1 min. Cycling was preceded by an initial denaturation step (94°C for 2 min) and followed by a final extension step (72°C for 10 min). The amplification products were then analyzed by 1% agarose gel electrophoresis. A grapevine elongation factor 1 (EF1) gene, amplified with primers 5′-TCAATCTGTCTAGGAAA GGAAG-3′ and 5′-GCGGGCAAGAGATACCTCAA-3′, was used as a control in the experiment.

Isolation of intact yeast vacuoles and vacuolar transport assays

Intact vacuoles were isolated as described by Ohsumi and Anraku (1981) with slight modifications, as described by Yamaguchi et al. (2003). The yeast mutant strain makes it possible to assess the contribution of this vacuolar sodium proton antiporter to ion transport by comparing transport in vacuoles isolated from the TY001 *nhx1* mutant and TY001 harboring *VvNHX1*. This was assayed by the measurement of rates of cation-dependent proton efflux using fluorescence quenching. The fluorescence quenching of acridine orange was used to monitor the establishment and dissipation of inside-acidic pH gradients between the vacuolar lumen and the assay buffer (Blumwald and Poole 1985, Yamaguchi et al. 2003). Changes of fluorescence with time were monitored on a PerkinElmer fluorescence spectrophotometer with an excitation wavelength of 495 nm and slit width of 2.5 nm, and an emission wavelength of 540 nm and 10 nm slit width with 1% of transmittance filter between the cuvette and the photomultiplier tube. Quantification of initial rates of acidification and fluorescence recovery was done with the FLWINLAB software package (PerkinElmer, Wellesley, MA, USA). Curves were normalized by setting the arbitrary fluorescence scale to 100. Rates of fluorescence recovery after the inhibition of the H^+-ATPase were normalized to the fluorescence quench attained in the assay just prior to the addition of the bafilomycin. Rates of transport of vacuoles transformed with the empty pDR196 were subtracted from the rates of transport of vacuoles isolated from the *S. cerevisieae* TY001 (Yamaguchi et al. 2003) transformed with *VvNHX1*-pDR196. Curves were fitted to the mean values of rates at each concentration and measured using KALEIDEGRAPH software (Synergy, Reading, PA, USA). Rates are reported as percentage quench per minute per milligram of protein.

Computer analysis

Sequence alignment and phylogenetic relationships were analyzed by the CLUSTAL X multiple sequence alignment algorithm (Thompson et al. 1997). The phylogenetic tree was drawn with TreeViewX (Zhai et al. 2002). Structural and topological predictions were done by TopPred2 (http://bioweb.pasteur.fr/seqanal/interfaces/toppred.html) and TMHMM (http://www.cbs.dtu.dk/services/TMHMM-2.0/) programs. Sequence analysis was performed with DNASTAR, and BLAST searches were performed on the NCBI platform (Altschul et al. 1990).

Acknowledgments

We would like to thank Dr. Barrieu François (Université de Bordeaux1, France) for kindly providing the grapevine cDNA library. This work was supported by a grant from the Ministry of Scientific Research, Technology and Competency Development in Tunisia, and by the Will W. Lester Endowment from the University of California.

References

Aharon, G.S., Apse, M.P., Duan, S.L., Hua, X.J. and Blumwald, E. (2003) Characterization of a family of vacuolar Na^+/H^+ antiporters in *Arabidopsis thaliana*. *Plant Soil* 253: 245–256.

Altschul, S.F., Gish, W., Miller, W., Myers, E.W. and Lipman, D.J. (1990) Basic local alignment search tool. *J. Mol. Biol.* 215: 403–410.

Apse, M.P., Aharon, G.S., Snedden, W.A. and Blumwald, E. (1999) Salt tolerance conferred by overexpression of a vacuolar Na^+/H^+ antiport in *Arabidopsis*. *Science* 285: 1256–1258.

Apse, M.P., Sottosanto, J.B. and Blumwald, E. (2003) Vacuolar cation/H^+ exchange, ion homeostasis, and leaf development are altered in a T-DNA insertional mutant of AtNHX1, the Arabidopsis vacuolar Na^+/H^+ antiporter. *Plant J.* 36: 229–239.

Asif, M.H., Dhawan, P. and Nath, P. (2000) A simple procedure for the isolation of high quality RNA from ripening banana fruit. *Plant Mol. Biol. Rep.* 18: 109–115.

Atanassova, R., Leterrier, M., Gaillard, C., Agasse, A., Sagot, E., Coutos-Thévenot, P. and Delrot, S. (2003) Sugar-regulated expression of a putative hexose transport gene in grape. *Plant Physiol.* 131: 326–334.

Benli, M., Döring, F., Robinson, D.G., Yang, X. and Gallwitz, D. (1996) Two GTPase isoforms, Ypt31p and Ypt32p, are essential for Golgi function in yeast. *EMBO J.* 15: 6460–6475.

Blumwald, E. (1987) Tonoplast vesicles for the study of ion transport in plant vacuoles. *Physiol. Plant.* 69: 731–734.

Blumwald, E. and Poole, R.J. (1985) Na^+/H^+ antiport in isolated tonoplast vesicles from storage tissue of *Beta vulgaris*. *Plant Physiol.* 78: 163–167.

Brini, F., Gaxiola, R.A., Berkowitz, G.A. and Masmoudi, K. (2005) Cloning and characterization of a wheat vacuolar cation/proton antiporter and pyrophosphatase proton pump. *Plant Physiol. Biochem.* 43: 347–354.

Burnette, W.N. (1981) 'Western blotting': electrophoretic transfer of proteins from sodium dodecyl sulfate–polyacrylamide gels to unmodified nitrocellulose and radiographic detection with antibody and radioiodinated protein A. *Anal. Biochem.* 112: 195–203.

Chang, S., Puryear, J. and Cairney, J. (1993) A simple and efficient method for isolating RNA from pine trees. *Plant Mol. Biol. Rep.* 11: 113–116.

Davies, C., Shin, R., Liu, , Thomas, M.R. and Schachtman, D.P. (2006) Transporters expressed during grape berry (*Vitis vinifera* L.) development are associated with an increase in berry size and berry potassium accumulation. *J. Exp. Bot.* 57: 3209–3216.

Fukuda, A., Nakamura, A., Tagiri, A., Tanaka, H., Miyao, A., Hirochika, H. and Tanaka, Y. (2004) Function, intracellular localization and the importance in salt tolerance of a vacuolar Na^+/H^+ antiporter from rice. *Plant Cell Physiol.* 45: 149–159.

Gaxiola, R.A., Rao, R., Sherman, A., Grisafi, P., Alper, S.L. and Fink, G.R. (1999) The *Arabidopsis thaliana* proton transporters, AtNhx1 and Avp1, can function in cation detoxification in yeast. *Proc. Natl Acad. Sci. USA* 96: 1480–1485.

Gietz, R.D., Schiestl, R.H., Willems, A.R. and Woods, R.A. (1995) Studies on the transformation of intact yeast cells by the LiAc/SS-DNA/PEG procedure. *Yeast* 11: 355–360.

Hamada, A., Shono, M., Xia, T., Ohta, M., Hayashi, Y., Tanaka, A. and Hayakawa, T. (2001) Isolation and characterization of a Na^+/H^+ antiporter gene from the halophyte *Atriplex gmelini*. *Plant Mol. Biol.* 46: 35–42.

Haseloff, J. (1999) GFP variants for multispectral imaging of living cells. *Methods Cell Biol.* 58: 139–151.

Hrazdina, G., Parsons, G.F. and Mattick, L.R. (1984) Physiological and biochemical events during development and ripening of grape berries. *Am. J. Enol. Vitic.* 35: 220–227.

Kanellis, A.K. and Roubelakis-Angelakis, K.A. (1993) Grape. *In* Biochemistry of Fruit Ripening. Edited by Seymour, G., Taylor, J. and Tucher, G. pp. 189–234. Chapman & Hall, London.

Laemmli, U.K. (1970) Cleavage of structural proteins during the assembly of the head of bacteriophage T4. *Nature* 227: 680–685.

Manning, K., Davies, C., Bowen, H. C. and White, P.J. (2001) Functional characterization of two ripening-related sucrose transporters from grape berries. *Ann. Bot.* 87: 125–129.

Mpelasoka, B.S., Schachtman, D.P., Treeby, M.T. and Thomas, M.R. (2003) A review on potassium nutrition in grapevines with special emphasis on berry accumulation. *Aust. J. Grape Wine Res.* 9: 154–168.

Numata, N., Petrecca, K., Lake, N. and Orlowski, J. (1998) Identification of a mitochondrial Na^+/H^+ exchanger. *J. Biol. Chem.* 273: 6951–9.

Ohsumi, Y. and Anraku, Y. (1981) Active transport of basic amino acids driven by a proton motive force in vacuolar membrane vesicles of *Saccharomyces cerevisiae*. *J. Biol. Chem.* 256: 2079–2082.

Ollat, N. and Gaudillere, J.P. (1996) Investigation of assimilate import mechanisms in berries of *Vitis vinifera* var. 'Cabernet Sauvignon'. *Acta Hort.* 427: 141–149.

Ohnishi, M., Fukada-Tanaka, S., Hoshino, A., Takada, J., Inagaki, Y. and Iida, S. (2005) Characterization of a novel Na^+/H^+ antiporter gene *InNHX2* and comparison of *InNHX2* with *InNHX1*, which is responsible for blue flower coloration by increasing the vacuolar pH in the Japanese morning glory. *Plant Cell Physiol.* 46: 259–267.

Pardo, J.M., Cubero, B., Leidi, E.O. and Quintero, F.J. (2006) Alkali cation exchangers: roles in cellular homeostasis and stress tolerance. *J. Exp. Bot.* 57: 1181–1199.

Picaud, S., Becq, F., Dedaldechamp, F., Ageorges, A. and Delrot, S. (2003) Cloning and expression of two plasma membrane aquaporins expressed during the ripening of grape berry. *Funct. Plant Biol.* 30: 621–630.

Pratelli, R., Lacombe, B., Torregrosa, L., Gaymard, F., Romieu, C., Thibaud, J.B. and Sentenac, H. (2002) A grapevine gene encoding a guard cell K^+ channel displays developmental regulation in the grapevine berry. *Plant Physiol.* 128: 564–577.

Quintero, F.J., Blatt, M.R. and Pardo, J.M. (2000) Functional conservation between yeast and plant endosomal Na^+/H^+ antiporters. *FEBS Lett.* 471: 224–228.

Rogiers, S.Y., Greer, D.H., Hatfield, J.M., Orchard, B.A. and Keller, M. (2006) Mineral sinks within ripening grape berries (*Vitis vinifera* L). *Vitis* 45: 115–123.

Rogiers, S.Y., Keller, M., Holzapfel, B.P. and Virgona, J.M. (2000) Accumulation of potassium and calcium by ripening berries on field vines of *Vitis vinifera* (L.) cv. Shiraz. *Aust. J. Grape Wine Res.* 6: 240–243.

Ruffner, H.P. (1982) Metabolism of tartaric and malic acids in *Vitis:* a review—part B. *Vitis* 21: 346–358.

Sottosanto, J.B., Gelli, A. and Blumwald, E. (2004) DNA array analyses of *Arabidopsis thaliana* lacking a vacuolar Na^+/H^+ antiporter: impact of AtNHX1 on gene expression. *Plant J.* 40: 752–771.

Terrier, N., Sauvage, F.X., Ageorges, A. and Romieu, C. (2001) Changes in acidity and in proton transport at the tonoplast of grape berries during development. *Planta* 213: 20–28.

Thompson, J.D., Gibson, T.J., Plewniak, F., Jeanmougin, F. and Higgins, D.G. (1997) The CLUSTAL_X windows interface: flexible strategies for multiple sequence alignment aided by quality analysis tools. *Nucleic Acids Res.* 25: 4876–4882.

Welch, R.M. (1986) Effects of nutrient deficiencies on seed production and quality. *Adv. Plant Nutr.* 2: 205–247.

Xia, T., Apse, M.P., Aharon, G.S. and Blumwald, E. (2002) Identification and characterization of a NaCl-inducible vacuolar Na^+/H^+ antiporter in *Beta vulgaris*. *Physiol. Plant.* 116: 206–212.

Yamaguchi, T., Aharon, G.S., Sottosanto, J.B. and Blumwald, E. (2005) Vacuolar Na^+/H^+ antiporter cation selectivity is regulated by calmodulin from within the vacuole in a Ca^{2+} and pH-dependent manner. *Proc. Natl Acad. Sci. USA* 102: 16107–16112.

Yamaguchi, T., Apse, M.P., Shi, H. and Blumwald, E. (2003) Topological analysis of a plant vacuolar Na^+/H^+ antiporter reveals a luminal C terminus that regulates antiporter cation selectivity. *Proc. Natl. Acad. Sci. USA* 100: 12510–12515.

Yamaguchi, T., Fukada-Tanaka, S., Inagaki, Y., Saito, N., Yonekura-Sakakibara, K., Tanaka, Y., Kusumi, T. and Iida, S. (2001) Genes encoding the vacuolar Na^+/H^+ exchanger and flower coloration. *Plant Cell Physiol.* 42: 451–461.

Yokoi, S., Bressan, R.A. and Hasegawa, P.M. (2002) Salt stress tolerance of plant. *JIRCAS Working Report* 000: 25–33.

Zhai, Y.F., Tchieu, J. and Saier, M.H. (2002) A web-based Tree View (TV) program for the visualization of phylogenetic trees. *J. Mol. Microbiol. Biotech.* 4: 69–70.

Zhang, H.X. and Blumwald, E. (2001) Transgenic salt-tolerant tomato plants accumulate salt in foliage but not in fruit. *Nature Biotech.* 19: 765–768.

(Received March 13, 2007; Accepted April 19, 2007)